

High-Resolution Photoelectron Spectroscopy and *ab initio* Quantum Chemistry

Stefan Willitsch, Andrea Wüest, and Frédéric Merkt*

Abstract: The resolution that can be achieved by photoelectron spectroscopy has been continually improved over the past 50 years and is now sufficiently high for the rovibronic energy level structure of polyatomic molecular cations to be measured accurately. Ionisation potentials, molecular constants, and in some cases the potential energy surfaces of both the neutral and the ionic states connected by the photoionising transitions can be extracted from photoelectron spectra and used to test *ab initio* quantum chemical calculations. *Ab initio* quantum chemistry represents an essential tool to assign photoelectron spectra and to rationalise the experimental observations. Because either the neutral or the ionised species, or even both, connected by a photoionising transition possesses at least one unpaired electron, photoelectron spectroscopy represents a very convenient method to study open-shell molecules. Unfortunately, much fewer highly accurate *ab initio* quantum chemical calculations have been reported on open-shell than on closed-shell molecules, and such calculations would be desired to assist in the interpretation of photoelectron spectra. This contribution illustrates the fruitful interplay between *ab initio* quantum chemistry and photoelectron spectroscopy with examples chosen from our recent work on the photoelectron spectra of the rare gas dimers and of small polyatomic hydrides and hydrocarbons. It also briefly reviews the experimental progress that makes it possible today to measure the fine and hyperfine structure in molecular ions by experimental techniques closely related to photoelectron spectroscopy.

Keywords: Ethyl radical · High-resolution photoelectron spectroscopy · Hyperfine structure of cations · Rare gas dimers and their cations

1. Introduction

Ab initio quantum chemistry and photoelectron spectroscopy have evolved hand in hand and matured as scientific disciplines for half a century. Continual improvements of the resolution of photoelectron spectroscopy have resulted in a need of increasingly accurate theoretical predictions of ionisation energies, molecular constants and potential energy surfaces for both neutral and charged species connected by photoionisation. The ability to resolve the electronic, vibrational and more recently the rotational and even spin-rotational and hyperfine structures in the photoelectron

spectra of molecules, and the desire to understand and model these structures have provided ample challenge to which *ab initio* quantum chemists have so far always responded rapidly.

In the early phase of this joint evolution, the combination of photoelectron spectroscopy and *ab initio* electronic structure calculations has been very successful in rendering the abstract concept of molecular orbitals accessible to all chemists [1–4]. Vertical ionisation potentials were interpreted as molecular orbital binding energies, and the vibrational intensity distributions were interpreted as arising from the overlap between the vibrational wave functions of the neutral and ionised molecules, thereby providing information on the potential energy surfaces and the chemical bonding of a wide range of molecules. Nowadays, photoelectron spectroscopy is increasingly used to determine the rovibronic energy level structure of polyatomic molecular ions and to derive information on the dynamical and thermochemical properties of molecular systems [5–12]. Attempts are also made to study the vibrational energy level structure of larger (biological) molecules [13].

The ways in which quantum chemistry can assist in the interpretation of photoelectron spectra are in many respects very similar to the ways it is used to interpret microwave, infrared or optical spectra, for instance by providing potential energy surfaces or molecular constants. Several needs, however, are specific to photoelectron spectroscopy:

- The correct interpretation of photoelectron spectra sometimes necessitates accurate calculations of adiabatic ionisation energies.
- Because of the open-shell nature of the neutral or the ionic state, the calculations must be applicable to molecules with unpaired electrons.
- The open-shell structure of the ionic or neutral species usually leads to a rich fine and hyperfine structure, which, when resolved, needs to be accounted for theoretically.
- The ionic species resulting from the photoionisation out of binding orbitals of the valence shell of stable and ‘rigid’ molecules such as CH_4 or C_2H_4 are often much less ‘rigid’ and undergo large amplitude motions and/or a complex

*Correspondence: Prof. F. Merkt
Physical Chemistry
ETH Hönggerberg, HCI
CH-8093 Zürich
Tel.: +41 1 632 43 67
Fax: +41 1 632 10 21
E-Mail: merkt@xuv.phys.chem.ethz.ch

tunnelling behaviour, necessitating careful investigations of extended regions of the potential energy surfaces.

In the work presented below, these specific needs of photoelectron spectroscopy are illustrated by examples taken from our recent investigations of the rare gas dimers and of small hydrides and hydrocarbons. Whereas the description of the neutral species in its ground neutral state, which possesses in most cases a well-behaved closed-shell electron configuration, rarely represents a problem for *ab initio* quantum chemistry, available calculations of the properties of the ionic species, or of electronically excited states, often lack the desired accuracy. Photoelectron spectroscopy would greatly benefit from more systematic *ab initio* calculations of open-shell molecules and ions.

2. Overview of Experimental Methods

The techniques used in our laboratory to record high-resolution photoelectron spectra are variants of pulsed-field-ionisation zero-kinetic-energy (PFI-ZEKE) photoelectron spectroscopy [14], in which the field ionisation of Rydberg states of high principal quantum number n located just below each ionisation threshold is monitored as a function of the wavenumber of a tuneable light source, typically a laser or a synchrotron [5][8][9]. The higher the resolution to be achieved, the more complex these variants become.

PFI-ZEKE photoelectron spectra can be routinely recorded at a resolution of 1 cm^{-1} by using simple electric field ionisation pulse sequences, such as a single pulsed electric field with an amplitude of $\approx 0.1\text{ V/cm}$ delayed by about $1\ \mu\text{s}$ with respect to the pulsed laser photoexcitation, or a sequence of two electric field pulses of opposite polarity (*e.g.* a first (discrimination) pulse of 0.1 V/cm followed by a second (detection) pulse of -0.2 V/cm). The discrimination pulse serves the purpose of field ionising the highest Rydberg states with $n \geq 350$ and of sweeping electrons produced by direct ionisation out of the measurement region. The PFI-ZEKE photoelectron spectra are then recorded by monitoring the field ionisation yield induced by the detection pulse as a function of the wavenumber of the radiation source. At a resolution of 1 cm^{-1} , the rotational structure of the photoelectron spectra of small polyatomic molecules with large rotational constants can be observed.

Resolving the complete rotational structure in the photoelectron spectrum of asymmetric top molecules and of larger polyatomic molecules necessitates the develop-

ment of electric field pulse sequences that are much more n selective. Pulse sequences consisting of a discrimination pulse of about 200 mV/cm followed by a series of detection pulses of opposite polarity and of gradually increasing amplitudes have so far proven to be the most n selective and to lead to the highest resolution (the best resolution achieved to date is 0.055 cm^{-1} [15]). The improved spectral resolution is well suited to study the rotational structure of larger molecules but is typically accompanied by a loss of sensitivity by a factor of about 5.

The methods described above do not have a resolution sufficient to determine the finest details of the energy level structure of molecular ions such as the hyperfine structure. Rather than trying to obtain such details by improving the selectivity of the field ionisation process, we have recently shown that very small energy splittings can be derived from high-resolution spectroscopic measurements in which the fine and/or the hyperfine structure of transitions to individual high Rydberg states with n in the range between 50 and 200 is resolved. Extrapolation to $n = \infty$ then yields the hyperfine structure of the cations. One technique we developed for this purpose, Rydberg state resolved threshold ionisation (RSRTI) spectroscopy [16], relies on the use of Fourier-transform-limited vacuum ultraviolet laser pulses with a bandwidth of $\approx 250\text{ MHz}$ [17] to record the fine and hyperfine structure of Rydberg states up to $n \approx 200$. The technique was used to measure the spin-rotational splittings of the rotational levels of NH_3^+ , to resolve the ground state tunnelling splitting in the photoelectron spectrum of NH_3 [18] and to determine the hyperfine structure of the $^{83}\text{Kr}^+$ ion [19]. A three orders of magnitude increase in resolution can further be achieved by using millimetre waves to record transitions between highly excited Rydberg states [20][21]. Extrapolation to the series limits leads to the determination of the hyperfine structure of ions at sub-MHz resolution.

RSRTI and millimetre wave spectroscopy of high Rydberg states require a reliable procedure to extrapolate the Rydberg series to their limit at $n = \infty$. Multichannel quantum defect theory is here the method of choice [22] and was used to determine the hyperfine structure of the $^2\text{P}_{3/2}$ ground state of $^{83}\text{Kr}^+$ [19] (see Fig. 1a) and the hyperfine structure of the $X\ ^2\Sigma_g^+$ ($v^+ = 0, N^+ = 1$) ground state of ortho H_2^+ (see Fig. 1b) by millimetre wave spectroscopy [23]. The latter structure was found to be in agreement with the theoretical predictions of Babb and Dalgarno [24]. H_2^+ represents one of the systems for which predictions by *ab initio* quantum chemistry have regularly been ahead of experimental results. Attempts at measuring the hyperfine structure of molecular ions by photoelectron spectroscopy and related tech-

niques would have been considered unrealistic ten years ago. Such measurements are now becoming possible and will hopefully stimulate the interest of theoretical chemists.

3. Examples

3.1. Photoelectron Spectroscopy of the Rare Gas Dimers

Our studies of the rare gas dimers (Rg_2) aim at a determination of the potential energy curves of the six low-lying electronic states of the cations (Rg_2^+) by photoelectron spectroscopy. Four of these states, labelled $\text{I}(1/2u)$, $\text{I}(3/2g)$, $\text{I}(1/2g)$, and $\text{I}(3/2u)$ (the Roman number indicates the dissociation limit and the labels in the parentheses give the value of Ω , the quantum number associated with projection of the electron angular momentum along the internuclear axis, and the gerade or ungerade symmetry of the electronic wavefunction), dissociate to a ground state atom ($\text{Rg}\ ^1\text{S}_0$) and a ground state ion ($\text{Rg}^+\ ^2\text{P}_{3/2}$). The other two states, labelled $\text{II}(1/2u)$ and $\text{II}(1/2g)$, dissociate to a ground state atom ($\text{Rg}\ ^1\text{S}_0$) and a spin-orbit excited ion ($\text{Rg}^+\ ^2\text{P}_{1/2}$) [25]. The potential energy curves of these electronic states are needed to predict the properties of larger ionic clusters (*e.g.* [26–29]), to characterise the radiative properties of the ions and quantify the absorption losses in ion lasers [30][31] and to model the potential energy curves of the Rydberg states of the rare gas dimers that are of importance in excimer lasers. Moreover, comparison of the potential energy curves of Ne_2^+ , Ar_2^+ , Kr_2^+ , and Xe_2^+ enables one to quantify the change in the electronic structure that arise as a consequence of the increasing spin-orbit interaction.

The experimental determination of the potential energy curves of the rare gas dimers represents an experimental challenge: the homonuclear dimers do not have a rotational or vibrational spectrum. Electronic spectra of transitions between the u and g states only reveal broad continuum structures. Photoelectron spectroscopy has so far represented the best approach to study the energy level structure of the dimer ions. However, because of limited resolution, only qualitative information on the ionic potential energy curves was known from experiment until recently. To determine reliable potential energy curves of the low-lying electronic states of the rare gas dimers, the complete information content of photoelectron spectra must be exploited:

- The vibrational intensity distributions are used to model the shape of the potential energy curves and, in favourable cases, to determine the equilibrium internuclear distances.
- Measurements of isotopic shifts are used to derive the absolute value of the vibrational quantum number.

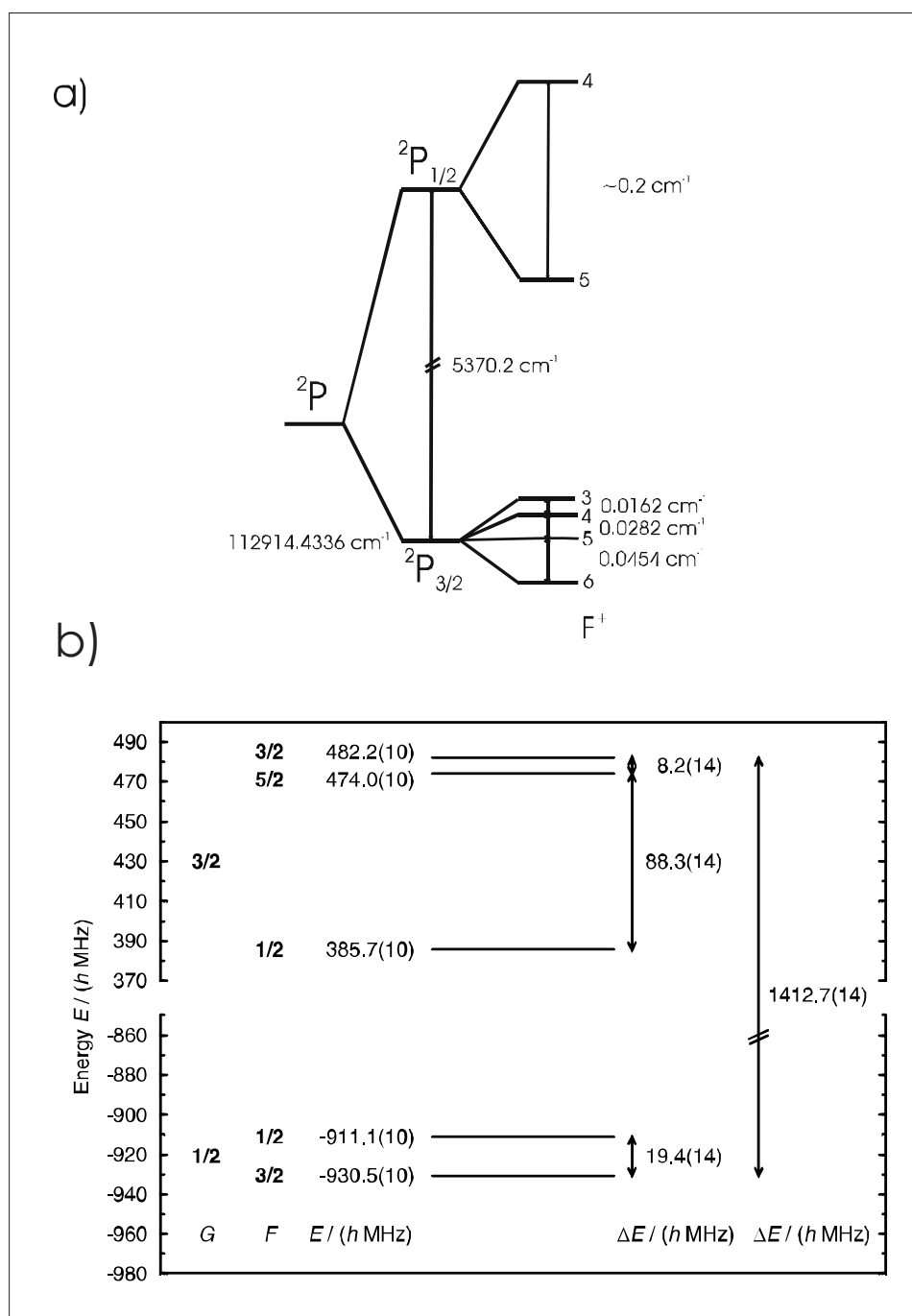


Fig. 1. Hyperfine structure of a) the $2P_{3/2}$ ground state and the $2P_{1/2}$ spin-orbit excited state of Kr^+ from [19] and b) the $X \ 2\Sigma_g^+$ ($v^+ = 0, N^+ = 1$) ground state of ortho H_2^+ from [23], as determined from an extrapolation of the hyperfine structure of Rydberg states using multichannel quantum defect theory.

- The rotational structure is exploited to determine internuclear distances.
- Finally, the fine structure of the rotational levels (Ω doublings and spin-rotational splittings) provide the information needed for an unambiguous assignment of the electronic symmetry [32].

In the case of the heavier dimers, the rotational constants are too small to be resolved, but the lack of information on the rotational structure can to some extent be compensated by *ab initio* quantum chemical calculations [33].

Not all ionic states are accessible from the ground neutral state because of unfavourable Franck-Condon factors, and it is imperative to record photoelectron spectra following both single-photon excitation from the ground state and resonance-enhanced multiphoton excitation *via* suitable intermediate electronic states. A Franck-Condon analysis of the vibrational intensity distributions often requires an independent determination of the potential energy curve of the neutral state from which ionisation occurs. So far our studies have led to measurements of the neutral ground state

potential energy curves of Ne_2 [34] and Xe_2 [35] for which no high-resolution spectra had been reported, of the potential energy curve of the $C \ 0_u^+$ excited state of Ne_2 [36] and of the 0_u^+ excited state of Kr_2 located below the $Kr \ 8^1S_0 + Kr^* \ (5p[1/2](J=0))$ dissociation limit [37], and of the potential energy curves of all six low-lying states of Ar_2^+ [25][32][38][39], of four states of Kr_2^+ [36][37][40] and five states of Xe_2^+ [41]. In each case, the potentials were determined by fitting analytical functions with adjustable parameters to the experimental level positions. The potentials were constructed so as to have the correct long-range behaviour and reproduce all experimental positions with an accuracy of better than 1 meV.

These studies offer an ideal opportunity for detailed comparison of the experimentally derived potential energy curves with those calculated *ab initio*. Selected experimental and *ab initio* potential energy curves of ground and excited states of the neutral dimers and of the dimer ions are compared in Fig. 2. The upper two panels compare experimental and *ab initio* potential energy curves of the neutral ground states of Ne_2 and Xe_2 . For Ne_2 the agreement between calculation and experiment is almost perfect and *ab initio* quantum chemistry has an accuracy comparable to the experiment [42]. In the case of Xe_2 , the calculations [43] underestimate the dissociation energy by almost 10% and predict a too large equilibrium distance. This discrepancy can be explained by the much larger number of electrons and the expected importance of relativistic effects.

A comparison of the *ab initio* [44] and experimental [25] potential energy curves of the lowest four electronic states of Ar_2^+ is presented in the bottom two panels of Fig. 2. The *ab initio* calculations capture the main features of the potential energy curves, in particular the double minimum of the $I(1/2g)$ state even though typical deviations between the two sets of curves amount to approximately 200 cm^{-1} . The deviations between *ab initio* and experimental curves are largest for the electronically excited states of the neutral dimers as is illustrated in the middle two panels of Fig. 2 with the example of the $C \ 0_u^+$ state of Ne_2 . The calculations [45] correctly predict the double minimum structure of the potential energy curve but the deviations between the measured [36] and calculated potential energy curves are significant.

The results of these comparisons are by no means surprising, as it is well known that the predictive power of *ab initio* quantum chemistry is reduced for open shell systems and rapidly decreases with the degree of electronic excitation and the number of electrons. The comparison nevertheless clearly shows where improvements in the

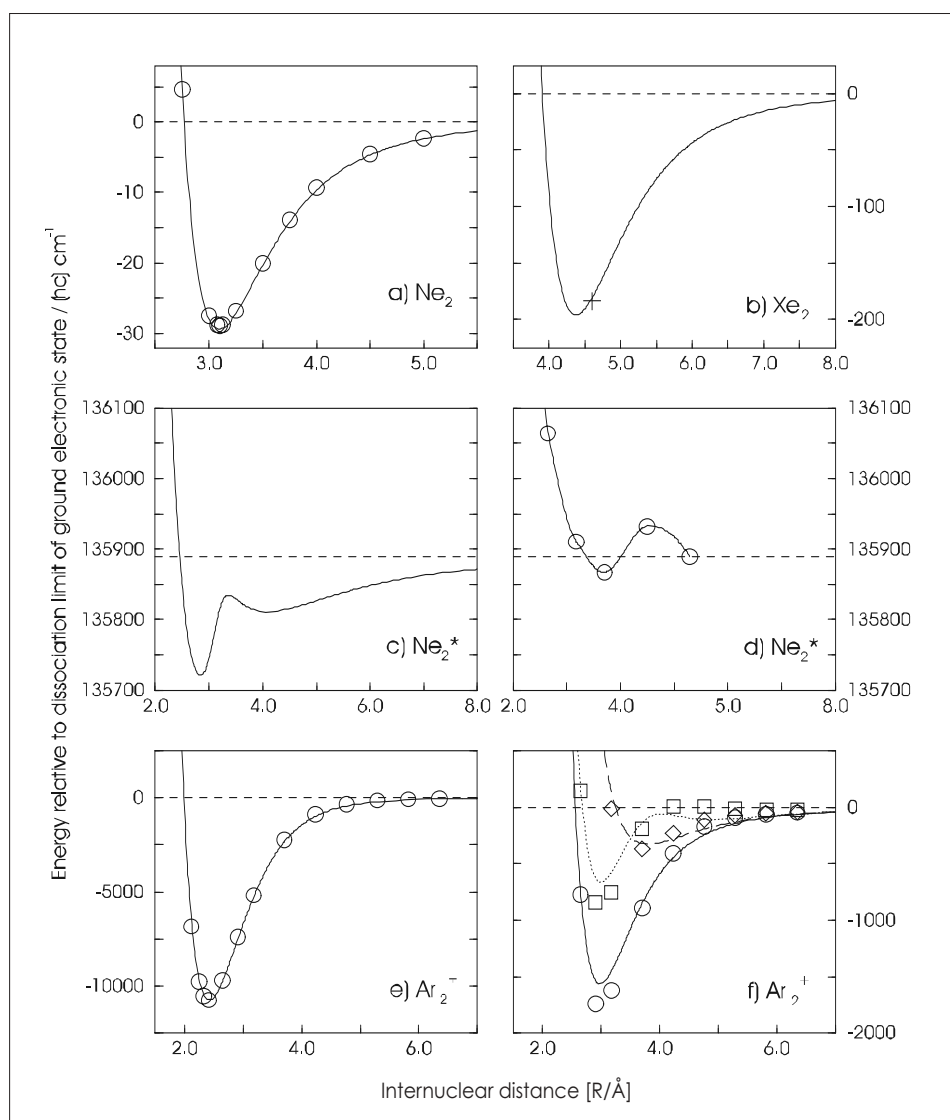


Fig. 2. Comparison of potential energy curves of the rare gas dimers determined from experimental data and by *ab initio* quantum chemical calculations: a) The $X\ 0_g^+$ ground neutral state of Ne_2 ; the experimental curve and the *ab initio* points are taken from [34] and [42], respectively. b) The $X\ 0_g^+$ ground neutral state of Xe_2 ; the experimental curve and the position of the potential minimum (indicated by a cross) calculated *ab initio* are taken from [35] and [43], respectively. c) Potential curve of the $C\ 0_u^+$ excited state of Ne_2 determined from experimental data [36]. d) *Ab initio* potential energy curve of the $C\ 0_u^+$ excited state of Ne_2 from [45]. The solid line connecting the *ab initio* points was determined by interpolation. e) Potential energy curve of the $I(1/2u)$ ground state of Ar_2^+ determined from experimental data [25] (full line) and *ab initio* calculations [44] (open circles). f) Potential energy curve of the $I(3/2g)$ (full line and open circles), $I(1/2g)$ (dotted line and squares) and $I(3/2u)$ (dashed line and diamonds) excited states of Ar_2^+ . The lines correspond to potential energy curves determined from experimental data [25] and the points to the results of *ab initio* calculations [44]. In a), b), e) and f) the curves have been shifted so that the origin of the energy scale corresponds to the first dissociation limit. In c) and d) the potential energy curves have been shifted so that the dissociation limit corresponds to the energy of the excited Ne dissociation product.

theoretical treatment would be particularly beneficial for the interpretation of photoelectron spectra.

3.2. Photoelectron Spectroscopy of Small Polyatomic Molecules

Photoelectron spectroscopy represents one of the most sensitive methods to obtain spectroscopic information on molecular radicals and cations. We have recently studied of small polyatomic hydro-

carbons and hydride molecules by high-resolution photoelectron spectroscopy. To access as wide a range of molecular systems as possible, a source of cold radicals based on laser photolysis in the high-pressure zone of a supersonic expansion was developed, and the feasibility of studying elusive species such as NH_2 , CH_2 , C_2H , and C_2H_5 by photoelectron spectroscopy was demonstrated [46–48]. The goals of these studies are to investigate the molecular photoioni-

sation dynamics in these systems, to obtain information on the large amplitude motions in the cationic states that arise from a loss of rigidity caused by the removal of a bonding electron, and to study the Jahn-Teller and Renner-Teller effects in the molecular cations. The Table presents a list of the molecules we have studied so far together with the specific phenomena we are studying in these molecules. An important byproduct of these investigations is the possibility to derive accurate values, also listed in the Table, of the adiabatic ionisation energies of the neutral hydrides and hydrocarbons that can be linked to thermochemical quantities such as enthalpies of formation and dissociation energies.

As an illustration of the power of high-resolution photoelectron spectroscopy to study small polyatomic cations, Fig. 3a shows the He I photoelectron spectrum (adapted from [54]) and Fig. 3b the PFI-ZEKE photoelectron spectrum of ethene (C_2H_4) [55]. In Fig. 3c, an expanded view of the first vibronic band is displayed. The spectrum was recorded at a resolution of $0.09\ \text{cm}^{-1}$ which is three orders of magnitude higher than the resolution achieved in the He I photoelectron spectrum. The three spectra displayed in Fig. 3 represent all experimental information known to date on the energy level structure of the ground electronic state of C_2H_4^+ and on the photoionisation dynamics of ethene. Striking features of the photoelectron spectra are the extended vibrational progressions associated with the torsional motion of the cation that were extensively discussed in [56] and used to show that C_2H_4^+ does not have a planar structure. Theoretical studies have provided insights into the mechanisms leading to the geometry change induced by removal of an electron from the highest occupied molecular orbital of ethene [57][58]. In particular, configuration interaction accompanied by vibronic coupling, was invoked as a general mechanism by which the structural constraints imposed on a molecule by a double bond are relaxed upon ionisation. High-resolution measurements such as that presented in Fig. 3 provide means to obtain detailed structural information on the cation and to study the effects of configuration interaction in the cation and on the photoionisation dynamics [55]. Configuration interaction results in the observation of (otherwise forbidden) photoionisation transitions to non-totally symmetric vibrational levels such as torsional levels with odd quanta of vibrational excitation. These transitions can easily be recognised in the spectra because of the different rotational structures that results from the photoionisation selection rules. The analysis of the spectra leads to the conclusion that the lowest two torsional levels are located below the barrier at the planar geometry sep-

Table. Overview of the hydrides and hydrocarbons studied by high-resolution photoelectron spectroscopy in Zurich in the past years. The Table also lists the first adiabatic ionisation energies of the neutral molecules and the motivations for these studies.

Molecule	Ionisation energy / cm^{-1}	Ref.	
CH_2	83772 ± 3	[47]	Quasilinearity and Renner-Teller effect
CH_4	101773 ± 35	[49]	Jahn-Teller effect
C_2H_2	91953.5 ± 0.5	[50]	Rovibronic structure, photoionisation dynamics
C_2H_4	84790.42 ± 0.23	[55]	Photoionisation dynamics, torsional motion
CH_2CO	77538.7 ± 0.7	[51]	Rovibronic structure
NH_2	100305.8 ± 0.8^a	[48]	Quasilinearity and Renner-Teller effect
NH_3	82158.751 ± 0.016	[18]	Spin-rotation splitting, photoionisation dynamics
ND_4	37490.7 ± 1.5	[52]	Photoionisation of a tetrahedral molecule
H_2O	101766.8 ± 1.2	[53]	Spin-rotation splitting

^aAdiabatic ionisation energy of the \bar{a}^+1A_1 ground electronic state of singlet NH_2^+

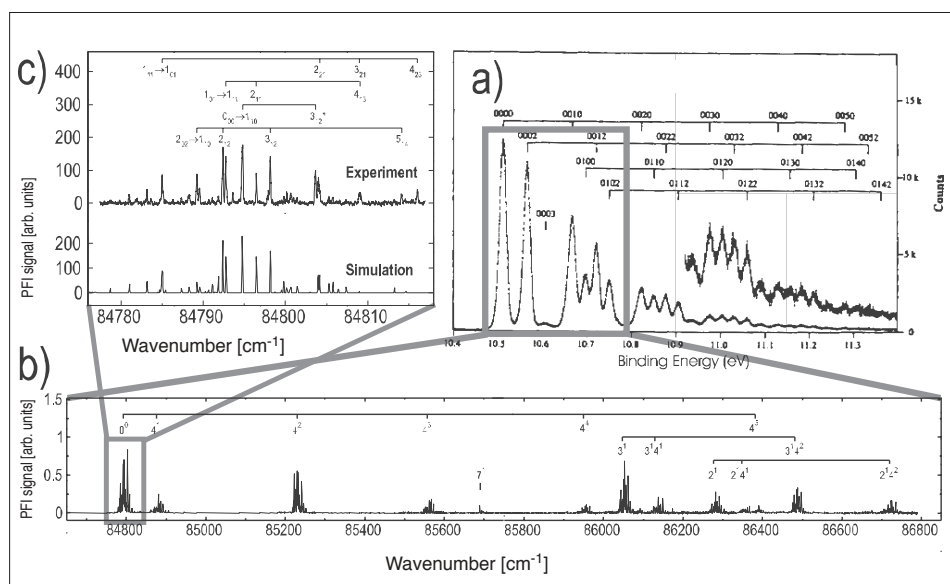


Fig. 3. a) He I photoelectron spectrum PFI-ZEKE photoelectron spectrum of the $\bar{X}^1A_g 0^0 \rightarrow \bar{X}^+ 2B_{3u} v_i^j$ transitions of C_2H_4 adapted from [54]. b) Survey of the PFI-ZEKE photoelectron spectrum recorded at a resolution of 0.6 cm^{-1} from [55]. c) PFI-ZEKE photoelectron spectrum of the lowest vibronic band recorded at a resolution of 0.09 cm^{-1} from [55].

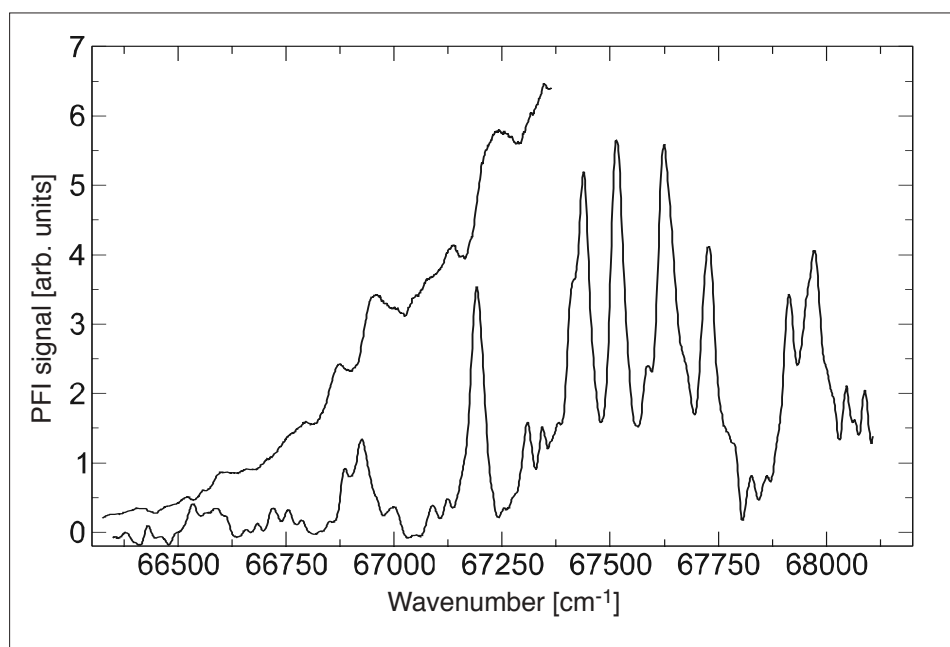


Fig. 4. Lower trace: Pulsed-field-ionisation zero-kinetic-energy photoelectron spectrum of the ethyl radical. Upper trace: Photoionisation spectrum of the ethyl radical (C_2H_5) recorded by monitoring the C_2H_5^+ ion signal as a function of the VUV laser wavenumber.

arating the two symmetric minima at $\pm 29^\circ$ along the torsional coordinate and constitute a tunnelling pair. Moreover, the tunnelling splitting was found to be insensitive to excitation of the CH_2 bending and C–C stretching modes, in contrast to chemical intuition [55].

There are several ways in which *ab initio* quantum chemical calculations could further our understanding of the spectrum: First, it could provide a quantitative description of the configurational mixing observed experimentally; second, it could provide an explanation for the apparent decoupling of the torsional motion from the C–C stretching and the CH_2 bending motion. Finally, the determination of the potential energy surface and a forward calculation of the rovibronic energy level structure might help in characterising the numerous vibrational interactions observed experimentally and in characterising the details of the torsional dynamics.

Whereas the assignment of photoelectron spectra such as that of ethene in Fig. 3 can be made on the basis of the well-resolved rotational structure, the assignment of more congested photoelectron spectra represents a difficult task. The problem is illustrated in Fig. 4 which shows the PFI-ZEKE photoelectron spectrum of the ethyl radical (C_2H_5) in the region of the onset of the first band. The attribution of the spectrum to the ethyl radical could be made on the basis of the photoionisation spectrum (upper trace in the figure) which shows clear steps at the ionisation thresholds corresponding to the positions of the lines in the PFI-ZEKE photoelectron spectrum. The gradual onset of the photoionisation signal indicates a significant change of geometry upon ionisation.

In the previous study of the He I photoelectron spectrum of the ethyl radical by Dyke and coworkers [59], no structure could be resolved in the first band. At higher resolution an unusually dense and irregular sequence of vibrational bands is observed (see Fig. 4), the assignment of which cannot be made without additional information. Photoionisation of the ethyl radical leads to the formation of the C_2H_5^+ cation for which both the classical $\text{H}_2\text{C}-\text{CH}_3$ and the non-classical bridged structure in which one of the H atoms is located above the C–C bond, have been predicted theoretically, the latter structure being more likely to be the most stable one [60]. Large amplitude motions accompanied by rapid exchange of the protons are expected to be dominant in the cation and could explain the dense and complex structure observed in the photoelectron spectrum. An *ab initio* calculation of the potential energy surfaces followed by forward calculation of the energy level structure as can be done successfully for small to medium sized polyatomic mole-

cules (e.g. [61–66]) appears at present to be the most promising route towards an assignment of the photoelectron spectrum of the ethyl radical.

We anticipate that the application of high-resolution photoelectron spectroscopy to progressively larger and more complex molecular systems will have to rely extensively on *ab initio* quantum chemical calculations and that photoelectron spectroscopy and *ab initio* quantum chemistry will continue to evolve hand in hand over the next 50 years.

Acknowledgements

We thank Prof. R. Signorell, Dr. A. Osterwalder, Dr. G.M. Greetham, Dr. U. Hollenstein, P. Rupper, R. Seiler, M. Sommovilla, H.-J. Wörner, O. Zehnder, K.G. de Bruin, H. Schmutz, M. Andrist, R. Gunzinger, Prof. T.P. Softley (Oxford), Prof. J.M. Dyke (Southampton) and Dr. C. Jungen (Orsay) for their participation in the research described in this article. This work is supported financially by the ETH Zürich and the Swiss National Science Foundation under project No. 200020-100050.

Received: March 15, 2004

- [1] D.W. Turner, C. Baker, A.D. Baker, C.R. Brundle, 'Molecular photoelectron spectroscopy', Wiley Interscience, London, **1970**.
- [2] J.H.D. Eland, 'Photoelectron spectroscopy', Butterworths, London, **1974**.
- [3] J.W. Rabalais, 'Principles of ultraviolet photoelectron spectroscopy', Wiley, New York, **1977**.
- [4] K. Kimura, S. Katsumata, Y. Achiba, T. Yamazaki, S. Iwata, 'Handbook of He I photoelectron spectra of fundamental organic molecules', Japan Scientific Societies Press, Tokyo, **1981**.
- [5] K. Müller-Dethlefs, E.W. Schlag, *Ann. Rev. Phys. Chem.* **1991**, *42*, 109.
- [6] F. Merkt, T.P. Softley, *Int. Rev. Phys. Chem.* **1993**, *12*, 205.
- [7] F. Merkt, *Ann. Rev. Phys. Chem.* **1997**, *48*, 675.
- [8] U. Hollenstein, R. Seiler, A. Osterwalder, M. Sommovilla, A. Wüest, P. Rupper, S. Willitsch, G.M. Greetham, B. Brupbacher-Gatehouse, F. Merkt, *Chimia* **2001**, *55*, 759.
- [9] C.-Y. Ng, *Ann. Rev. Phys. Chem.* **2002**, *53*, 101.
- [10] T. Wright, *Annu. Rep. Prog. Chem., Sect. C* **2002**, *98*, 375.
- [11] I. Fischer, *Int. J. Mass. Spectrom.* **2002**, *216*, 131.
- [12] T.P. Softley, *Int. Rev. Phys. Chem.*, in press.
- [13] C.E.H. Dessent, K. Müller-Dethlefs, *Chem. Rev.* **2000**, *100*, 3999.
- [14] G. Reiser, W. Habenicht, K. Müller-Dethlefs, E.W. Schlag, *Chem. Phys. Lett.* **1988**, *152*, 119.
- [15] U. Hollenstein, R. Seiler, H. Schmutz, M. Andrist, F. Merkt, *J. Chem. Phys.* **2001**, *115*, 5461.
- [16] R. Seiler, U. Hollenstein, G.M. Greetham, F. Merkt, *Chem. Phys. Lett.* **2001**, *346*, 201.
- [17] U. Hollenstein, H. Palm, F. Merkt, *Rev. Sci. Instrum.* **2000**, *71*, 4023.
- [18] R. Seiler, U. Hollenstein, T.P. Softley, F. Merkt, *J. Chem. Phys.* **2003**, *118*, 10024.
- [19] H.J. Wörner, U. Hollenstein, F. Merkt, *Phys. Rev. A*, **2003**, *68*, Art. Nr. 032510.
- [20] F. Merkt, H. Schmutz, *J. Chem. Phys.* **1998**, *108*, 10033.
- [21] F. Merkt, A. Osterwalder, *Int. Rev. Phys. Chem.* **2002**, *21*, 385.
- [22] C. Jungen (Ed.), 'Molecular applications of quantum defect theory', Institute of Physics Publishing, Bristol, **1996**.
- [23] A. Osterwalder, A. Wüest, F. Merkt, C. Jungen, to be published.
- [24] J.F. Babb, A. Dalgarno, *Phys. Rev. A* **1992**, *46*, R5317.
- [25] A. Wüest, F. Merkt, *J. Chem. Phys.* **2004**, *120*, 638.
- [26] K. Stephan, T.D. Märk, *Phys. Rev. A* **1985**, *32*, 1447.
- [27] F.Y. Naumkin, D.J. Wales, *Mol. Phys.* **1998**, *93*, 633.
- [28] N.L. Doltsinis, P.J. Knowles, *Mol. Phys.* **1998**, *94*, 981.
- [29] R. Kalus, I. Páidarová, D. Hrivňák, P. Paška, F.X. Gadéa, *Chem. Phys.* **2003**, *294*, 141.
- [30] J.G. Eden, *IEEE J. Sel. Top. Quantum Electron.* **2000**, *6*, 1051.
- [31] J.J. Ewing, *IEEE J. Sel. Top. Quantum Electron.* **2000**, *6*, 1061.
- [32] P. Rupper, F. Merkt, *J. Chem. Phys.* **2002**, *117*, 4264.
- [33] T.-K. Ha, P. Rupper, A. Wüest, F. Merkt, *Mol. Phys.* **2003**, *101*, 827.
- [34] A. Wüest, F. Merkt, *J. Chem. Phys.* **2003**, *118*, 8807.
- [35] A. Wüest, U. Hollenstein, K.G. de Bruin, F. Merkt, *Can. J. Chem.*, accepted for publication.
- [36] A. Wüest, Ph. D. Thesis, Diss. ETH Nr. 15310, ETH Zurich, **2003**.
- [37] A. Wüest, P. Rupper, F. Merkt, *Mol. Phys.* **2001**, *99*, 1941.
- [38] R. Signorell, F. Merkt, *J. Chem. Phys.* **1998**, *109*, 9762.
- [39] P. Rupper, F. Merkt, *Mol. Phys.* **2002**, *100*, 3781.
- [40] R. Signorell, U. Hollenstein, F. Merkt, *J. Chem. Phys.* **2001**, *114*, 9840.
- [41] P. Rupper, O. Zehnder, F. Merkt, to be published.
- [42] R.J. Gdanitz, *Chem. Phys. Lett.* **2001**, *348*, 67.
- [43] P. Slavíček, R. Kalus, P. Paška, I. Odvárková, P. Hobza, A. Malijevský, *J. Chem. Phys.* **2003**, *119*, 2102.
- [44] F.X. Gadéa, I. Páidarová, *Chem. Phys.* **1996**, *209*, 281.
- [45] F. Grein, S.D. Peyerimhoff, *J. Chem. Phys.* **1987**, *87*, 4684.
- [46] S. Willitsch, J.M. Dyke, F. Merkt, *Helv. Chim. Acta* **2003**, *86*, 1152.
- [47] S. Willitsch, F. Merkt, *J. Chem. Phys.* **2003**, *118*, 2235.
- [48] S. Willitsch, J.M. Dyke, F. Merkt, *Mol. Phys.*, accepted for publication.
- [49] R. Signorell, F. Merkt, *Faraday Discussions* **2000**, *115*, 205.
- [50] P. Rupper, F. Merkt, *Rev. Sci. Instrum.* **2004**, *75*, 613.
- [51] S. Willitsch, A. Haldi, F. Merkt, *Chem. Phys. Lett.* **2002**, *353*, 167.
- [52] R. Signorell, H. Palm, F. Merkt, *J. Chem. Phys.* **1997**, *106*, 6523.
- [53] F. Merkt, R. Signorell, H. Palm, A. Osterwalder, M. Sommovilla, *Mol. Phys.* **1998**, *95*, 1045.
- [54] D.M.P. Holland, D.A. Shaw, M.A. Hayes, L.G. Shpinkova, E.E. Rennie, L. Karlsson, P. Baltzer, B. Wannberg, *Chem. Phys.* **1997**, *219*, 91.
- [55] S. Willitsch, U. Hollenstein, F. Merkt, *J. Chem. Phys.* **2004**, *120*, 1761.
- [56] J.E. Pollard, D.J. Trevor, J.E. Reutt, Y.T. Lee, D.A. Shirley, *J. Chem. Phys.* **1984**, *81*, 5302.
- [57] H. Köppel, W. Domcke, L.S. Cederbaum, W. von Niessen, *J. Chem. Phys.* **1978**, *69*, 4252.
- [58] H. Köppel, L.S. Cederbaum, W. Domcke, S.S. Shaik, *Angew. Chem. Int. Ed. Engl.* **1983**, *22*, 210.
- [59] J.M. Dyke, A.R. Ellis, N. Keddar, A. Morris, *J. Phys. Chem.* **1984**, *88*, 2565.
- [60] W. Quapp, D. Heidrich, *J. Mol. Struct. (Theochem)* **2002**, *585*, 105.
- [61] H. Lin, W. Thiel, S.N. Yurchenko, M. Carvajal, P. Jensen, *J. Chem. Phys.* **2002**, *117*, 11265.
- [62] B. Fehrensen, D. Luckhaus, M. Quack, M. Willeke, T.R. Rizzo, *J. Chem. Phys.* **2003**, *119*, 5534.
- [63] O.L. Polyansky, A.G. Császár, S.V. Shirin, N.F. Zobov, P. Barletta, J. Tennyson, D.W. Schwenke, P.J. Knowles, *Science* **2003**, *299*, 539.
- [64] S.M. Colwell, S. Carter, N.C. Handy, *Mol. Phys.* **2003**, *101*, 523.
- [65] P. Jensen, M. Brumm, W.P. Kraemer, P.R. Bunker, *J. Mol. Spectrosc.* **1995**, *172*, 194.
- [66] X.G. Wang, T. Carrington, *J. Chem. Phys.* **2003**, *119*, 101.